The effect of tube dimensions on optimized pressure and force loading paths in tube hydroforming process [†]

S. M. H. Seyedkashi[1], H. Moslemi Naeini[1], G. H. Liaghat[1], M. Mosavi Mashadi[2], M. Mirzaali[1],
K. Shojaee[3] and Y. H. Moon[4,*]

[1]*Department of Mechanical Engineering, Tarbiat Modares University, Tehran, Iran*
[2]*Department of Mechanical Engineering, University of Tehran, Tehran, Iran*
[3]*Department of Electrical and Computer Engineering, University of Tehran, Tehran, Iran*
[4]*School of Mechanical Engineering, Pusan National University, Busan, Korea*

Abstract

The precise control of internal pressure and axial force loading paths significantly affects the final product quality. In this study, the effect of tube dimensions on the pressure and force loading paths in tube hydroforming process is investigated by using simulated annealing optimization method linked to a commercial finite element code. The optimized loading paths, obtained for different tube geometries with a constant expansion ratio, are then compared. The effects of initial diameter and wall thickness on shape conformation, optimal internal pressure and axial force (or feed) are discussed on the basis of optimal loading paths. Several guidelines in prediction and determination of tube hydroforming parameters are obtained by optimization analysis.

Keywords: Tube hydroforming process; Loading path optimization; Simulated annealing method

---

1. Introduction

Tube hydroforming (THF) technology is growing fast in automotive industry due to its great advantages in comparison with similar forming processes. In recent years, many studies have been performed to determine the process parameters in order to produce a defect-free product. Koc and Altan [1] determined the process limits and parameters for hydroforming by plasticity, membrane and thin/thick walled tube theories. Manabe and Amino [2] confirmed the parameters affecting wall thickness distribution of the hydroformed tubes. Kridli et al. [3] discussed the effect of thickness and corner radius on corner filling and thickness distribution of the hydroformed tube into a square die cross-section. Aydemir et al. [4] designed an adaptive method to obtain a more efficient control on tube hydroforming process. Kang et al. [5] discussed the tube size effect on hydroformability of a vehicle bumper rail section. Yang and Ngaile [6] developed an analytical model based on deformation theory to predict hydroformed shape, corner fill, wall thinning and forming pressure. In all cases, the pressure and feed loading paths were not comprehensively optimized.

Due to the combinatory conditions of loadings in tube hydroforming process, it is difficult to determine the accurate amounts of internal pressure and axial feed by theoretical equations or conventional methods. Different optimization methods have been used or proposed by researchers to improve loading conditions in THF process [7-12]. In this paper, simulated annealing (SA) algorithm -written in MATLAB and linked to the nonlinear finite element code ANSYS/LS-DYNA [13]- is used to predict the optimal pressure and axial force loading paths in THF process [14]. The final goal is to find the effects of tube diameter and wall thickness on the optimized internal pressure and axial force loading paths. Nine different cases -shown in Table 1- are discussed in this research. To avoid the effects of expansion ratio and corner radii, these parameters are kept constant in all cases as 31.5% and 5 mm, respectively. Diameter-to-thickness ratio (D_i/t) is different in each case according to the given dimensions. D_i is the tube initial diameter and D_f final bulge diameter. Tube is made of ASTM C11000 copper alloy [15]. Friction coefficient between die and tube is assumed to be a constant of 0.05. Material properties of tube –obtained by tensile test- are defined in Table 2. Experiments are performed to verify the results of the first case in order to assess the validity of the optimization method and the obtained results.

Table 1. Tube dimensions in each case.

Thickness \ Diameter	$D_i = 15.87,$ $D_f = 20.87$	$D_i = 20.00,$ $D_f = 26.30$	$D_i = 25.00,$ $D_f = 32.88$
0.63	$D_i/t = 25.19,$ $D_f/t = 33.13$	$D_i/t = 31.74,$ $D_f/t = 41.75$	$D_i/t = 39.68,$ $D_f/t = 52.19$
1.00	$D_i/t = 15.87,$ $D_f/t = 20.87$	$D_i/t = 20.00,$ $D_f/t = 26.3$	$D_i/t = 25.00,$ $D_f/t = 32.88$
1.50	$D_i/t = 10.58,$ $D_f/t = 13.91$	$D_i/t = 13.33,$ $D_f/t = 17.53$	$D_i/t = 16.66,$ $D_f/t = 21.92$

Table 2. Material properties of tube.

Yield stress, σ_y (MPa)	130	Density, ρ (g/cm³)	8.9
Ultimate tensile stress, σ_{uts} (MPa)	285	Poisson ratio, υ	0.32
Maximum elongation, ε (%)	28	Strength coefficient, K (MPa)	365
Young modulus of elasticity, E (GPa)	85	Strain hardening exponent, n	0.185

2. Optimization method and verification

Optimization is one of the most interesting topics in research and industry. In recent decades, different optimization methods and tools have been proposed and developed. The common goal of these techniques is to find the best way to obtain the optimal responses for different problems. Optimization leads to the higher quality products and less production costs. The utilized optimization method in this research is called "Simulated Annealing" technique, which is categorized as a metaheuristic. Metaheuristic is a computational method that optimizes a problem by iteratively trying to improve a solution with regard to a given measure of quality. Metaheuristic can search very large spaces of solutions. However, it might not always find the best solution, but it is guaranteed to find a good solution in a reasonable time. Application of Simulated Annealing (SA) in optimization of engineering problems is widely increased [16] but to the best knowledge of the authors, it is the first time used in a forming process [17]. The idea of simulated annealing was proposed by Metropolis et al. [18] and used for optimization problems by Kirkpatrick et al. [19]. Optimization concept of SA is inspired by cooling process of a heated metal. Free movements of molecules gradually decrease by temperature reduction, and the crystalline structure of metal forms homogeneously so that the system is approximately in thermodynamic equilibrium all the time [20, 21]. In the simulated annealing method, each point of the search space is assumed to be analogous to a state of the physical annealing system, and the function E (which is to be minimized) is analogous to the internal energy of the system in that state.

The first module of SA algorithm is the definition of annealing schedule. Getting entrapped in local minima is avoided upon proper selection of annealing schedule which is defined by four parameters; initial temperature, freezing temperature, cooling function (the amount of temperature reduction at each step as cooling proceeds) and Markov chain num-

ber (the number of iterations at each temperature). Finding the optimal values and definitions for these parameters is totally problem dependent, which must be defined on an empirical basis. In other words, the main disadvantage, that is common in stochastic local search algorithms, is that there are no choices of these parameters good for all problems. If the initial temperature is too low, it may enter a metastable state. Freezing temperature is zero and Markov chain number is selected 15. Several types of cooling function have been reported in the literature [22]. In this paper, a kind of logarithmic cooling function is selected as $T(k) = T(k-1)/[1+\ln(k+1)]$ [17]. This function updates the temperature at each iteration, and is very accurate but a little bit slow.

The second module of SA algorithm is the acceptance probabilities of iterations in the search process. Based on the acceptance condition, if the energy changes are negative ($\Delta E \leq 0$), the new configuration will be accepted. But if the changes are positive ($\Delta E > 0$), it is accepted with a probability given by the Boltzmann distribution function $\exp(-\Delta E/T)$. It potentially saves the method from becoming stuck at local optima. This process is repeated sufficient times to give good sampling statistics for the current temperature. Then the temperature is decremented by cooling function, and the entire process is repeated until a frozen state is achieved [23, 24].

Optimization process is very time-consuming. However, there are several ways to decrease the number of needed iterations. Determination of initial pressure and axial force has a great effect on the total run time of the program. However, for restricting the search space in order to decrease the total run time, it is required to properly define upper and lower bounds for internal pressure and axial feed. More precise these estimations are, the sooner the results converge to the optimized one. In this research, the values for internal pressure are calculated by simple theoretical equations as Eqs. (1) and (2) [25]. P_{yield} is the pressure needed to start plastic deformation, while $P_{calibration}$ is the maximum pressure required to form the sharp corners. $P_{calibration}$ multiplied by 1.2, and P_{yield} are used as the pressure upper and lower bounds, respectively. The average of upper and lower bounds is determined as the initial value for internal pressure. Moreover, to prevent wrinkling during the process, the axial force upper bound is limited to critical axial force for wrinkling, F_{cr}, as Eq. (3) [1].

$$P_{yield} = \sigma_y \frac{2}{(D_i/t) - 1} \tag{1}$$

$$P_{calibration} = \frac{2}{\sqrt{3}} \sigma_f \ln\left[\frac{(r/t)}{(r/t) - 1}\right] \tag{2}$$

$$F_{cr} = \frac{4\pi}{3}(E_t)t^2 \tag{3}$$

where t is the initial tube thickness, D_i the tube initial diameter, r the corner radius, σ_f the flow stress (usually ultimate tensile strength is used instead), σ_y the yield strength, and E_t the tangent modulus.
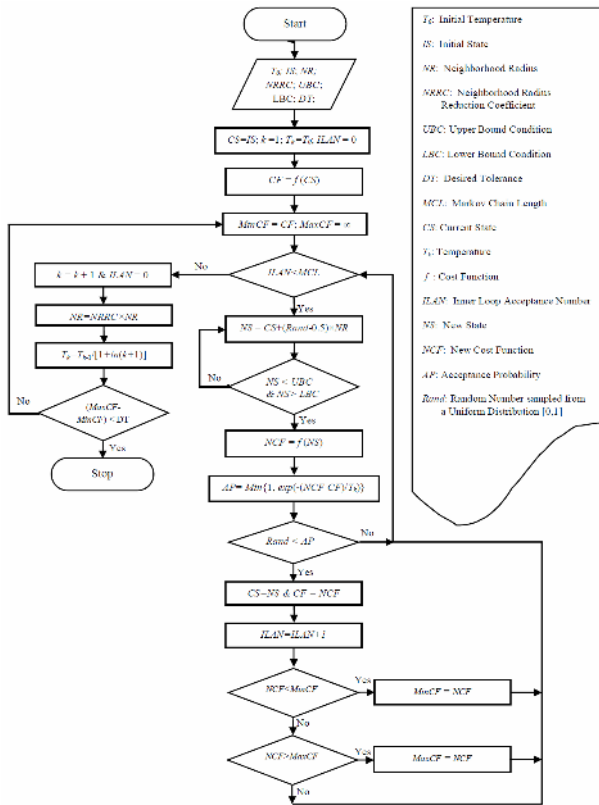
In order to apply SA for an optimization problem, the real

Fig. 1. SA algorithm's flowchart.

Fig. 2. Thinning percentage vs. tube length in comparison of FEA and Experimental results.

process parameters should be analogized with the SA definitions. The algorithm tries to minimize the energy to optimize the problem. THF process should produce fully formed non-defective parts with minimum wall thinning and without any defects such as wrinkling or buckling. Therefore, the gap between the nodes of tube and die is analogized as "Energy" which has to be minimized in this paper. Hence, the maximum conformation of the tube with final geometry at the end of forming process is assumed as a "goal function" in the algorithm. This condition is checked by calculating the distance between the opposite nodes of the tube and die. Gradients of pressure and axial force versus time diagrams are assumed to be the input variables. In each step, by considering a new set for gradients of pressure and axial force as input variables, a new energy (distance between nodes) is obtained in finite element analysis.

An axisymmetric element PLANE162 is used for part meshing. Die is assumed as a perfectly rigid body and tube material follows power law plasticity rule. The material is assumed to be isotropic and the effect of strain rate is neglected. Failure criterion is determined by von-Mises stress and the tube final thickness. Maximum thinning of 28% is considered as a failure criterion in finite element simulations. Moreover, the maximum von-Mises stress must not be higher than the ultimate tensile strength of material. Fig. 1 shows the optimization algorithm flowchart for tube hydroforming process.
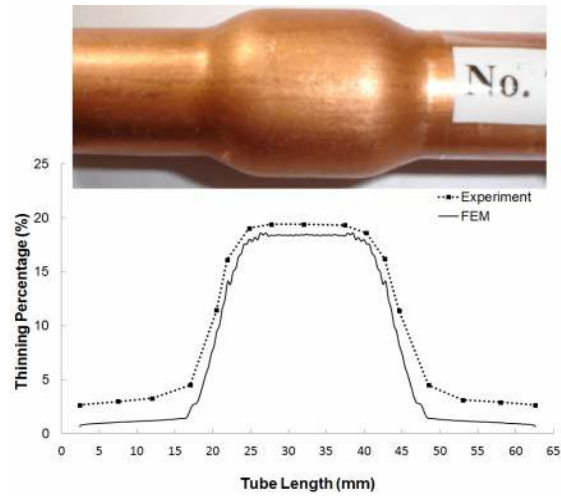
Based on the optimized pressure obtained from SA code, experiments are performed for the first case. The thinning percentages obtained by finite element analysis (FEA) and experiments are compared in Fig. 2. Two graphs have similar trends in which maximum thinning will happen in the middle of the tube where the maximum bulge occurs. It is observed that there is 1% difference between finite element and experimental results in the middle of the tube where the least contact friction exists, while it increases up to 1.65% along the tube ends. This difference is due to the frictional conditions in the experiments, since full lubrication is assumed in finite element analyses (coefficient of friction = 0.05). Higher frictions and the roughness of die and tube surfaces always result in higher thinning percentages. It should also be noted that the precision of optimized values is four decimal digits. So the more precise control system will give more reliable results. A detailed comparative study for validation of this method in tube hydroforming process is presented in Ref. [17].

3. Results and discussion

Fig. 3 shows the goal function versus successful iterations for all cases. Note that the number of total iterations is more in each case, but according to the "Fault detection" of the algorithm, unsuccessful simulations are automatically eliminated. It is shown that the cases in which their thickness is lower show the best tube to die shape conformation, while those with higher thickness have the least shape conformation. Lower goal function value shows a lower tube to die node distance, hence better shape conformation. It can be concluded that with a constant initial diameter, corner fillet and expansion ratio, the increase in thickness reduces the shape conformation, while with a constant wall thickness, the increase in diameter results in better shape conformation. In other words, the shape conformation is proportional to the diameter to thickness ratio (D_i/t). Eqs. (4) and (5) are two common equations used to predict the
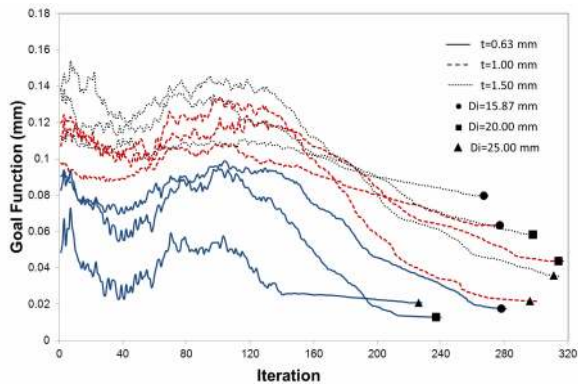
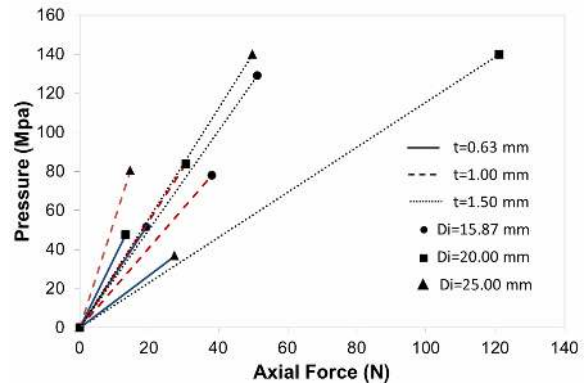Fig. 3. Comparison of goal function vs. iterations.
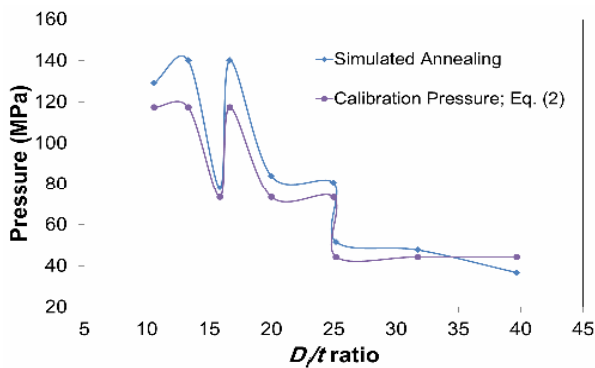

Fig. 5. Optimized loading paths for all cases.

Fig. 4. Comparison of theoretical results with simulated annealing.
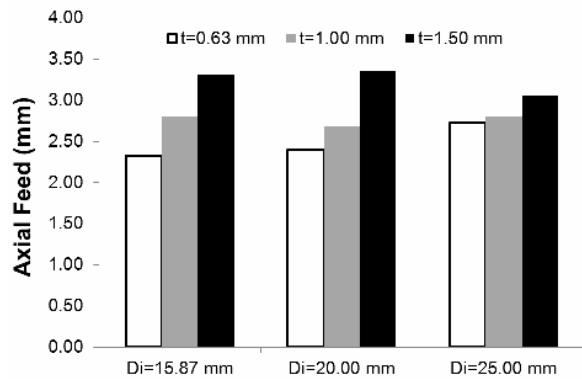

Fig. 6. Comparison of optimum axial feeds.

bursting (forming) pressure. Bursting pressure $P_{bursting}$ is the pressure needed to form the tube bulge. Eq. (4) relates the forming pressure to the initial diameter to thickness ratio (D_i/t) [1], while Eq. (5) relates it to the final diameter to thickness ratio (D_f/t) [25]. Although these equations confirm the relation of pressure to D/t ratio, they do not provide its relation to the shape conformation, which is reversed. It should be reminded that these equations are proven for simple geometries, and application of axial force would change the amount of pressure at different stages of the forming process.

$$P_{bursting} = \sigma_{uts} \frac{2}{(D_i/t)-1} \qquad (4)$$

$$P_{bursting} = \sigma_{uts} \frac{4}{(D_f/t)-1} \qquad (5)$$

Fig. 4 compares the pressures predicted by Eq. (2) with SA results. Note that Eqs. (4) and (5) can only be used in free bulging or where bi-linear or multi-linear pressure application is performed, because they do not take into account the important role of corner radius. Fig. 4 shows that the trend of the optimum pressures -predicted by SA method- is the same as theoretical predictions; though it shows higher values are required. This difference is due to the frictional conditions and axial feeding.

Fig. 5 shows the optimum loading path for each case. It in-

dicates the effect of increase in the initial tube thickness and diameter on the optimized pressure-force loading paths. The increase of the thickness has a considerable effect on both required internal pressure and axial force. On the other hand, with a constant thickness, the increase of diameter has more effect on axial force in comparison with internal pressure. It should be noted that with the same thickness, increasing of axial force does not necessarily increase the amount of axial feed. It depends on tube diameter and counter pressure on the punches. Fig. 6 approves this issue too. It is seen that for the cases with the same thickness, the amount of axial feed has a small change by increasing the diameter. Fig. 6 compares the optimal axial feed needed for each case. It illustrates that if the final geometry (initial diameter D_i, final diameter D_f and corner radius r) is the same, more axial feeding should be applied for a ticker tube to be fully formed. It can be concluded by comparing Fig. 5 with Fig. 6 that the effect of thickness on needed axial feed is higher than the effect of initial diameter. Theoretical methods are also proposed to calculate the amount of needed axial feed in the process [26], but they assume volume constancy, hence not reliable enough. Use of an optimization tool will ensure the manufacturing of a product without any failures such as wrinkling, buckling or bursting.

Fig. 7 shows the thinning distribution in tube length for all cases. The maximum allowable thinning is 28%, and the optimized path tries to keep it the lowest possible. This figure
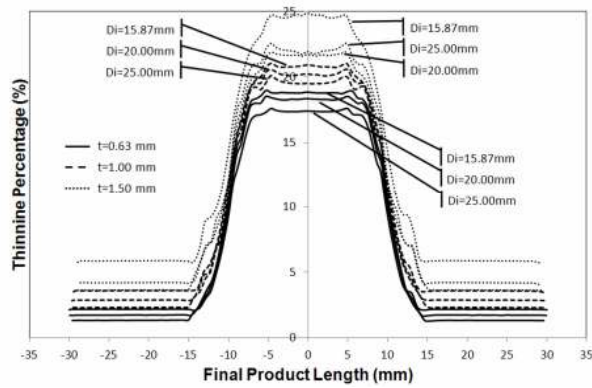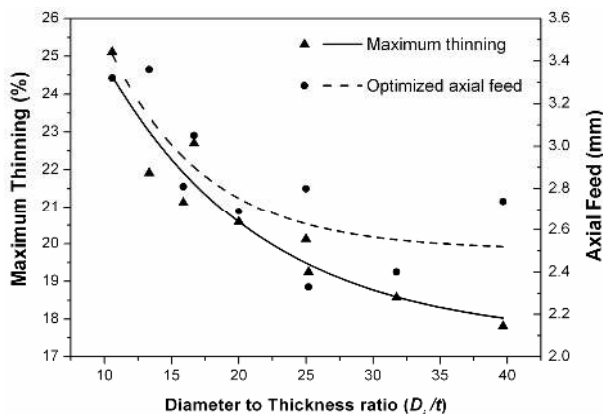
Fig. 7. Thinning distribution in tube length.

Fig. 8. The effect of D_i/t ratio on maximum thinning percentage and axial feed.

briefly describes the effect of changes in thickness and diameter on shape conformation. The highest shape conformation and the least thinning percentage are obtained for the cases with lower thicknesses. Ticker tube produces a part with higher strength, but less shape conformation and higher weight and cost. Therefore, special care should be taken when designing the product according to the working conditions. The maximum thinning occurs for the case with the shortest diameter and largest thickness, while the minimum thinning has happened for the case with the largest diameter and shortest thickness. It can be seen that the thinning percentage is considerably decreased by reduction of the thickness, while it is slightly increased by reduction of initial diameter -in a constant thickness. Fig. 8 illustrates the effect of initial diameter to thickness ratio on the maximum thinning percentage and axial feed. It shows both of them follow a reduction trend with increase in D_i/t ratio. It can be concluded by comparison of Fig. 7 with Fig. 8 that the effect of thickness on thinning and feeding is also higher than the initial diameter.

4. Conclusions

A novel optimization method is used for tube hydroforming process based on Simulated Annealing algorithm. This method can be used as a fast and reliable design tool for determination of hydroforming parameters and loading paths. Because of the complex combinatory condition of loads in tube hydroforming, theoretical methods are not capable of determining the optimal internal pressure and axial force (feed). Based on the results obtained by this method for optimization of internal pressure and axial force in tube hydroforming, several guidelines are provided to help the designers estimate the appropriate pressure and force loading paths.

- With a constant initial diameter, corner fillet and expansion ratio, the increase of thickness results in less shape conformation.

- With a constant wall thickness, the increase in diameter results in better shape conformation.

- With a constant diameter, the increase in thickness should be compensated by increasing both internal pressure and axial force.

- With a constant thickness, the increase in diameter has more effect on axial force in comparison with internal pressure.

- The effect of thickness on needed axial feed and pressure is higher than that of initial diameter.

References

[1] M. Koc and T. Altan, Prediction of forming limits and parameters in the tube hydroforming process, *International Journal of Machine Tools and Manufacture*, 42 (2002) 123-138.

[2] K. Manabe and M. Amino, Effects of process parameters and material properties on deformation process in tube hydroforming, *Journal of Materials Processing Technology*, 123 (2002) 285-291.

[3] G. T. Kridli, L. Bao, P. K. Mallick and Y. Tian, Investigation of thickness variation and corner filling in tube hydroforming, *Journal of Materials Processing Technology*, 133 (2003) 287-296.

[4] A. Aydemir, J. H. P de Vree, W. A. M. Brekelmans, M. G. D. Geers, W. H. Sillekens and R. J. Werkhoven, An adaptive simulation approach designed for tube hydroforming processes, *Journal of Materials Processing Technology*, 159 (2005) 303-310.

[5] S.-J. Kang, H.-K. Kim and B.-S. Kang, Tube size effect on hydroforming formability, *Journal of Materials Processing Technology*, 160 (2005) 24-33.

[6] Ch. Yang and G. Ngaile, Analytical model for planar tube hydroforming: Prediction of formed shape, corner fill, wall thinning, and forming pressure, *International Journal of Mechanical Science*, 50 (2008) 1263-1279.

[7] K. J. Fann and P. Y. Hsiao, Optimization of loading conditions for tube hydroforming, *Journal of Materials Processing Technology*, 140 (2003) 520-524.

[8] B. Li, T. J. Nye and D. R. Metzger, Multi-objective optimization of forming parameters for tube hydroforming process based on the Taguchi method, *International Journal of Ad-*

vanced Manufacturing Technology, 28 (2006) 23-30.

[9] M. Imaninejad, G. Subhash and A. Loukus, Loading path optimization of tube hydroforming process, *International Journal of Machine Tools and Manufacture*, 45 (2005) 1504-1514.

[10] K. Manabe, M. Suetake, H. Koyama and M. Yang, Hydroforming process optimization of aluminum alloy tube using intelligent control technique, *International Journal of Machine Tools and Manufacture*, 46 (2006) 1207-1211.

[11] M. Jansson, L. Nilsson and K. Simonsson, On process parameter estimation for the tube hydroforming process, *Journal of Materials Processing Technology*, 190 (2007) 1-11.

[12] N. Abedrabbo, M. Worswick, R. Mayer and I. van Riemsdijk, Optimization methods for the tube hydroforming process applied to advanced high-strength steels with experimental verification, *Journal of Materials Processing Technology*, 209 (2009) 110-123.

[13] J. O. Hallquist, *LS-Dyna 970 Theoritical Manual*, Livermore Software Technology Corporation, Livermore, California, (1998).

[14] M. Mirzaali, G. H. Liaghat, H. Moslemi Naeini, S. M. H. Seyedkashi and K. Shojaee, Optimization of tube hydroforming process using simulated annealing algorithm, *Procedia Engineering*, 10 (2011) 3012-3019.

[15] S. H. Lee, J. Y. Lim, H. Utsunomiya, K. Euh and S. Z. Han, Microstructure and mechanical properties of a Cu-Fe-P copper alloy sheet processed by differential speed rolling, *Korean Journal of Metals and Materials*, 48 (2010) 942-950.

[16] R. Chibante, *Simulated annealing theory with application*, Sciyo Press, Rijeka, Croatia, (2010) 1-16.

[17] M. Mirzaali, S. M. H. Seyedkashi, G. H. Liaghat, H. Moslemi Naeini, K. Shojaee and Y. H. Moon, Application of simulated annealing method to pressure and force loading optimization in tube hydroforming process, *International Journal of Mechanical Sciences*, 55 (2012) 78-84.

[18] N. Metropolis, A. Rosenbluth, M. Rosenbluth, A. Teller and E. Teller, Equation of state calculations by fast computing machines, *Journal of Chemical Physics*, 21 (1953) 1087-1092.

[19] S. Kirkpatrick, C. D. Gelatt and M. P. Vecchi, Optimization by simulated annealing, *Science*, 220 (1983) 671-680.

[20] Y. G. Kim, Y. G. Ko, D. H. Shin, C. S. Lee and S. Lee, Effect of annealing temperature on dynamic deformation behavior of ultra-fine-grained aluminium alloys fabricated by equal channel angular pressing, *Korean Journal of Metals and Materials*, 46 (2010) 563-571.

[21] S. H. Lee, D. J. Yoon, K. Euh, S. H. Kim and S. Z. Han, Annealing characteristics of oxygen free copper sheet processed by differential speed rolling, *Korean Journal of Metals and Materials*, 48 (2010) 77-84.

[22] M. M. Keikha, Improved simulated annealing using momentum terms, proc. of the Second International Conference on Intelligent Systems, *Proc. of Modelling and Simulation (ISMS)*, Cambodia (2011) 44-48.

[23] M. J. Dashti, K. G. Shojaee, S. M. H. Seyedkashi and M. T. Behnam, Novel simulated annealing algorithm in order to optimal adjustment of digital PID controller, *Proc. of the 11th International Conference on Control, Automation, Robotics and Vision (ICARCV)*, Singapore (2010) 1766-1771.

[24] K. G. Shojaee, N. Mollai, S. M. H. Seyedkashi and M. M. Neshati, New simulated annealing algorithm for quadratic assignment problem, *proc. of the 4th International Conference on Advanced Engineering Computing and Applications in Sciences (ADVCOMP)*, Italy (2010) 87-99.

[25] Y. Aue-U-Lan, G. Ngaile and T. Altan, Optimizing tube hydroforming using process simulation and experimental verification, *Journal of Materials Processing Technology*, 146 (2004) 137-143.

[26] N. Asnafi and A. Skogsgårdh, Theoretical and experimental analysis of stroke-controlled tube hydroforming, *Materials Science and Engineering: A*, 279 (2000) 95-110.

S. M. Hossein Seyedkashi is currently a PhD candidate at department of mechanical engineering, Tarbiat Modares University, Tehran, Iran. His research interests are tube and sheet hydroforming, laser forming and optimization.

Hassan Moslemi Naeini is a professor at department of mechanical engineering, Tarbiat Modares University, Tehran, Iran since 2000. His research interests are roll forming, hydroforming and laser forming.

YoungHoon Moon is a professor at school of mechanical engineering, Pusan National University, Republic of Korea. His research interests are development of advanced processing technology and process analysis.